ARTICLE

Comparative Investigation of Mo(CO)$_6$ Adsorption on Clean and Oxidized Si(111) Surfaces

Zhi-quan Jiang*, Wei-xin Huang*

Hefei National Laboratory for Physical Sciences at the Microscale, CAS Key Laboratory of Materials for Energy Conversion, Department of Chemical Physics, University of Science and Technology of China, Hefei 230026, China

Mo(CO)$_6$ adsorption on the clean, oxygen-precovered and deeply oxidized Si(111) surfaces was comparatively investigated by high-resolution electron energy loss spectroscopy. The downward vibrational frequency shift of the C−O stretching mode in adsorbed Mo(CO)$_6$ illustrates that different interactions of adsorbed Mo(CO)$_6$ occur on clean Si(111) and SiO$_2$/Si(111) surfaces, weak on the former and strong on the latter. The strong interaction on SiO$_2$/Si(111) might lead to the partial dissociation of Mo(CO)$_6$, consequently the formation of molybdenum subcarbonyls. Therefore, employing Mo(CO)$_6$ as the precursor, metallic molybdenum could be successfully deposited on the SiO$_2$/Si(111) surface but not on the clean Si(111) surface. A portion of the deposited metallic molybdenum is transformed into the MoO$_3$ on the SiO$_2$/Si(111) surface upon heating, and the evolved MoO$_3$ finally desorbs from the substrate upon annealing at elevated temperatures.

Key words: Molybdenum hexacarbonyl, SiO$_2$/Si(111), Interaction, High-resolution electron energy loss spectroscopy

I. INTRODUCTION

The adsorptive and reactive properties of organo-metallic compounds on catalyst surfaces have recently attracted increasing attention. Group VIB hexacarbonyls render suitable as precursors for selective metal deposition on surfaces, providing an effective approach to prepare supported metal catalysts [1, 2]. The metals in the carbonyls are normally in the zero-valent state and the CO ligands are stable, noncondensable gas themselves, so that thermal decomposition of metal carbonyls can, in principle, eliminate CO from the carbonyl molecules, leaving the metal alone on the surface. Thermal decomposition of W(CO)$_6$ and Fe(CO)$_5$ has been investigated and subsequently mechanistic studies of thermal decomposition was connected with chemical vapor deposition processes [3−8]. Employing these metal carbonyls as the precursor, the metallic components can be deposited on substrates.

Silica-supported molybdenum-based catalysts has received extensive applications in fields such as olefin metathesis, epoxidation of alkenes [9, 10]. Mo(CO)$_6$ is usually used as an effective metal-containing precursor for the preparation of molybdenum species [4, 11−14]. Therefore it is very meaningful to investigate the ad-

sorption and decomposition of Mo(CO)$_6$ on the catalyst supports. So far, the adsorption and reaction of molybdenum hexacarbonyl on γ-alumina [15, 16] and alumina thin films [17−24] have been extensively investigated. Moreover, those on silica have also been studied by means of various techniques, including infrared spectroscopy, temperature-programmed decomposition (TPDE) and Raman spectroscopy, and the formation of different subcarbonyl species was observed on the oxide surfaces [25, 26]. It has been reported that decarbonylation began when Mo(CO)$_6$ was adsorbed onto the silica, and dehydroxylation of the support during calcination facilitated the formation of subspecies of Mo(CO)$_6$ [25]. However, the nonconductivity of the silica support in practical catalysis hampers the investigation of surface chemistry by a variety of ultrahigh vacuum (UHV) analytical techniques. The interaction between Mo(CO)$_6$ and the Si(111)-7×7 surface has been investigated at low temperatures under UHV conditions [27−32]. It was deduced from the thermal desorption spectroscopy (TDS), high-resolution electron energy loss spectroscopy (HREELS) and IRAS (infrared reflection absorption spectroscopy) results that Mo(CO)$_6$ was molecularly adsorbed on the clean Si(111) surface [27−29]. Furthermore, it was verified by direct photoelectronic excitation, hot electron attachment or thermal effect that the partial and entire decomposition of adsorbed Mo(CO)$_6$ occurred on Si(111) [28−32]. Nanometer-sized dot structures were reported to be fabricated on Si(111)-7×7 surfaces by

---

*Authors to whom correspondence should be addressed. E-mail: jzhiquan@ustc.edu.cn, huangwx@ustc.edu.cn, Tel.: +86-551-3600435, FAX: +86-551-3600437

scanning tunneling microscopy (STM) induced local decomposition of $Mo(CO)_6$ molecules and bonding of the decomposition products to the surface [31]. As far as we know, there has been no relevant reports about the behavior of $Mo(CO)_6$ on thin SiO_2 film, which would be a better system to mimic practical catalysis than on the clean Si(111) surface.

In this work, $Mo(CO)_6$ adsorption was comparatively investigated on the clean, oxygen-precovered and deeply oxidized Si(111) surfaces. $Mo(CO)_6$ adsorbs molecularly on the clean and oxygen-precovered Si(111) surfaces at cryogenic temperature, as evidenced by the C−O stretching vibrational frequencies at 2073 and 2076 cm^{-1}, respectively. The adsorbed $Mo(CO)_6$ on SiO_2/Si(111) exhibits a C−O stretching vibrational frequency at 2040 cm^{-1}, lower than those on Si(111) and O/Si(111). It clearly suggests that $Mo(CO)_6$ interacts strongly with SiO_2/Si(111), but very weakly with clean Si(111) and O/Si(111). Therefore, dosing $Mo(CO)_6$ onto SiO_2/Si(111) at 700 K leads to molybdenum deposition; however, no molybdenum was detected by Auger electron spectroscopy (AES) on Si(111) and O/Si(111) substrates after the same process. The deposited metallic molybdenum, derived from entire thermal decomposition of $Mo(CO)_6$, is further oxidized by the SiO_2/Si(111) substrate into the MoO_3, which desorbs from the substrate upon annealing at elevated temperatures. In this work, we offers a deep insight into the interaction and adsorptive properties of $Mo(CO)_6$ on various substrates. An easy way was also provided to prepare a model surface of molybdenum-modified oxide, which is free from the surface carbon contaminant.

II. EXPERIMENTS

Experiments were carried out in an UHV system with a base pressure of 20 nPa, which was described in detail elsewhere [13, 14]. In brief, the UHV system was equipped with facilities for AES and HREELS, and an ion gun for cleaning the sample. The AE spectra were recorded through a hemispherical energy analyzer, with an incident electron energy of 3 keV at a pass energy of 150 eV. The HREEL spectra were collected on an ELS-22 instrument in the specular direction, with an incident angle of 60° and a primary incident electron beam energy of 5.0 eV. The spectral resolution was approximately 100 cm^{-1} on a clean surface, with a slight decrease on the oxidized surface. An *n*-type Si(111) wafer, with a resistivity of 8−20 mΩ·cm, was fixed via some small clamps onto a Ta foil, which was supported on the sample holder with two Ta wires. The sample temperature was monitored by a chromel/alumel thermocouple pressed on the Si(111) surface by an insulating clamp. The sample could be either cooled down to 100 K with liquid nitrogen, or resistively heated up to 1000 K. The Si(111) sample was rinsed in 10% HF solution, then in distilled water and ethanol, and subse-
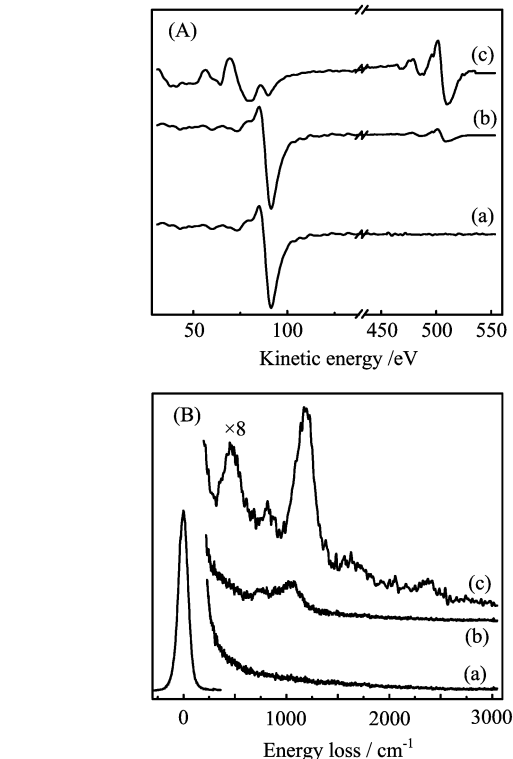
FIG. 1 (A) Auger electron spectra and (B) HREEL spectra of (a) the clean Si(111) surface, (b) the clean Si(111) surface with O_2 exposure of 10 L at room temperature, and (c) the SiO_2/Si(111) surface.

quently introduced into the UHV chamber. The Si(111) surface was cleaned by standard procedures, including oxidation, Ar$^+$ sputtering and annealing at a high temperature, until no contaminants could be detected by AES and HREELS. $Mo(CO)_6$ (Aldrich Chemical Company, Inc., 98%) was used after further purification in the manifold via several freeze-pump-thaw cycles. Prior to each exposure, the $Mo(CO)_6$ vapor was prepared by pumping on the solid for several minutes. $Mo(CO)_6$ was fed through a capillary array doser, which was aimed directly at the sample, thus preventing an undesirable rise in the background pressure of $Mo(CO)_6$. The exposure was determined by integrating the pressure increase as a function of time, without correction for the local dose enhancement and gauge sensitivity. All exposures determined in this way were specified hereafter as Langmuirs (1 L=133 µPa·s).

III. RESULTS AND DISCUSSION

Figure 1 illuminates a series of AES and HREELS for the Si(111) surface with different oxidative degrees. Only one characteristic feature appears at 91 eV in Fig.1(a) for the clean Si(111) surface, corresponding to the LVV Auger transition. When the Si(111) substrate is exposed to 10 L oxygen at room temperature, the

silicon Auger feature does not change; only a new feature develops at approximately 508 eV, corresponding to the KLL transition of adsorbed oxygen. The ideal Si(111) surface is dominantly terminated with a surface Si atom having one unsaturated broken bond. The presence of this dangling bond makes it feasible for O$_2$ to dissociatively adsorb on the Si(111) surface. The silicon LVV transition does not change its Auger feature upon oxygen exposure, indicating that the Si−Si bond is not broken. According to the results of Hollinger and Himpsel [33], the coverage of atomic oxygen in our case is estimated to be approximately 0.8 ML.

Then the Si(111) surface was oxidized under rigorous conditions (the sample at 1000 K was exposed to 0.2 Pa O$_2$ for 60 min). The new and distinct Auger transitions emerge at 59, 63, and 76 eV, characteristic of the silicon-oxygen tetrahedron. It clearly indicates that silicon oxide film has formed upon such rigorous treatment. The thickness of the oxide film on the Si(111) substrate can be estimated by the Auger features during the oxidation process. It is assumed that the Auger electrons of the silicon substrate reduce their intensity when traversing the oxide film. The attenuation of the Auger intensity follows an exponential law [34]:

$$I_{\mathrm{Si}}(d) = I_{\mathrm{Si}}(0) \exp\left(-\frac{d}{\lambda}\right) \tag{1}$$

where d is the thickness of the oxide film on the Si(111) surface, $I_{\mathrm{Si}}(0)$ and $I_{\mathrm{Si}}(d)$ are the Si LVV Auger intensities from the clean and oxidized surfaces, respectively, and λ is the escape depth of 91 eV electrons passing through the oxide film (λ=0.65 nm [34]). Therefore, the thickness of the oxide film is estimated to be approximately 1.5 nm, as deduced from the intensity ratio of the silicon and silicon oxide signals (in (a) in Fig.1(A)). This model surface is henceforth denoted as the SiO$_2$/Si(111) surface. Under 0.1 mPa of H$_2$ ambient, the SiO$_2$/Si(111) surface has no reduction sign till 900 K. At the same time, the obvious formation of the surface hydroxyl can not be deduced from the HREELS measurements. It suggests that this SiO$_2$/Si(111) model surface remains stable within a relatively wide temperature range, and is tolerant to a reductive ambient.

Figure 1(B) shows a series of HREELS for the Si(111) surface with different oxidative degrees. When 10 L of O$_2$ was dosed onto the clean Si(111) surface at room temperature, two vibrational peaks develop at 1021 and 751 cm^{-1}, corresponding to the antisymmetric and symmetric stretching modes of the Si−O bonds [35, 36]. The absence of an apparent loss feature at approximately 1230 cm^{-1}, which is a reasonable candidate for the oxygen-oxygen stretching vibration when bonded to silicon [35], indicates almost no molecular oxygen adsorption on Si(111) at room temperature. It clearly suggests that dissociative adsorption occurs on clean Si(111) upon molecular oxygen exposure at room
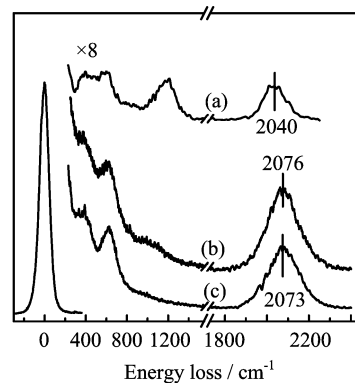
FIG. 2 HREEL spectra of Mo(CO)$_6$ with 5 L exposure adsorbed on (a) the clean Si(111) surface, (b) the 10 L O$_2$ preadsorbed Si(111) surface, and (c) the SiO$_2$/Si(111) surface at 100 K.

temperature, only adsorbed atomic oxygen on the silicon surface. Additionally, Lee and Kang concluded in their density functional calculations that the molecular state is unstable on Si(111)-7×7: an O$_2$ molecule spontaneously dissociates without any barrier [37, 38]. This vibrational feature characteristic of atomic oxygen adsorption clearly suggests that the Si−Si bonds are not broken upon 10 L of O$_2$ exposure at room temperature, in good accordance with the Auger results. After the Si(111) surface was subjected to oxidation in 0.2 Pa O$_2$ ambient at 1000 K for 60 min, huge changes of the vibrational feature occur in the HREEL spectrum. Three distinct vibrational signals at 462, 818, and 1191 cm^{-1}, and relatively weak peaks at 1630 and 2378 cm^{-1} emerge on the substrate. The signals at 818 and 1191 cm^{-1} are attributed to the symmetric and antisymmetric stretching modes of the Si−O bonds, respectively. The vibrational feature at 462 cm^{-1} is assigned to the bending mode of the Si−O−Si group. The weak peaks at 1630 and 2378 cm^{-1} are ascribed to the combinative and double losses of the fundamental losses, respectively [35]. Therefore, the SiO$_2$/Si(111) model surface has formed upon high-temperature oxidation. The SiO$_2$/Si(111) model surface offers the advantage of using AES and HREELS to scrutinize the surface chemistry of real silica supports, while avoiding the charging problems that would normally occur when electron-based techniques are used with insulating samples.

Mo(CO)$_6$ adsorption were all performed at cryogenic temperature, since the sticking coefficient of Mo(CO)$_6$ is very low on solid surfaces at room temperature. Figure 2 displays HREEL spectra of 5 L Mo(CO)$_6$ adsorbed on a clean Si(111) surface, 10 L O$_2$ precovered Si(111) surface and the SiO$_2$/Si(111) model surface at 100 K. On clean Si(111), three vibrational peaks appear at 2073, 389, and 626 cm^{-1} upon Mo(CO)$_6$ exposure. These peaks are attributed to the C−O stretching (ν_6), Mo−CO stretching (ν_8), and Mo−CO bend (ν_7),

respectively, in accordance with the vibrational modes for $Mo(CO)_6$ molecules in the gas phase [39−41]. It illustrates that $Mo(CO)_6$ adsorbs molecularly on the clean Si(111) surface at 100 K, agreeing well with previous reports [27, 32]. On O/Si(111), the adsorbed $Mo(CO)_6$ exhibits the vibrational signals at 2076, 387, and 627 cm^{-1}, similar to those on clean Si(111). These observations demonstrate that the presence of adsorbed oxygen on Si(111) does not exert much influence on the reactivity to $Mo(CO)_6$ and that $Mo(CO)_6$ also molecularly adsorbs on O/Si(111). On these two substrates, molecular $Mo(CO)_6$ bonds to the surface via the oxygen atom in the carbonyl group of hexacarbonyls.

On the SiO$_2$/Si(111) model surface, the intense signals appear at 395, 588, and 2040 cm^{-1} upon 5 L exposure of $Mo(CO)_6$ at 100 K, corresponding to the Mo−CO stretching, Mo−CO bend and C−O stretching modes, respectively. The feature at 1199 cm^{-1}, corresponding to the antisymmetric stretching vibration of the Si−O bonds, is still visible after $Mo(CO)_6$ adsorption. In comparison with those of $Mo(CO)_6$ on the clean and oxygen-precovered Si(111) surfaces, the C−O stretching vibrational frequency of $Mo(CO)_6$ on the SiO$_2$/Si(111) surface undergo downshifts by as much as 42 cm^{-1}. It demonstrates that the adsorption of $Mo(CO)_6$ on SiO$_2$/Si(111) is quite different from those on clean Si(111) and O/Si(111). A likely reason for the observed vibrational frequency downshifts might be an interaction of adsorbates with the polar silica substrate. Owing to a finite dipole moment along the surface normal, the polar oxide surfaces may exhibit higher activities than the non-polar surfaces [42, 43]. Furthermore, such strong interaction between adsorbed $Mo(CO)_6$ and SiO$_2$/Si(111) might result in partial dissociation of adsorbates on SiO$_2$/Si(111), which could also contribute to the downward vibrational frequency shift of the C−O stretching mode in adsorbed carbonyls. It has been reported by Ying and Ho [44] and So and Ho [45] that the vibrational frequencies of the Mo−CO stretching (ν_8) and bend (ν_7) and C−O stretching (ν_6) modes all shifted downward after adsorbed $Mo(CO)_6$ was partially decomposed. $Mo(CO)_6$ adsorbed molecularly on both Ag(111) and the basal plane of graphite, and dissociatively on both surfaces after low-power UV irradiation ($\lambda<360$ nm); at the meanwhile, the C−O vibrational feature moved from 2000 cm^{-1} to 1984 cm^{-1} after photodissociation [45]. Therefore, the large vibrational frequency downshifts in our case might also be due to partially dissociative adsorption of $Mo(CO)_6$ on the SiO$_2$/Si(111) surface, consequently the formation of molybdenum subcarbonyls. Decarbonylation was reported to begin when $Mo(CO)_6$ was adsorbed onto the real silica support, and subspecies of partially-decarbonylated molybdenum carbonyls were detected by diffuse reflectance IR spectroscopy [25]. The molybdenum subcarbonyls bond to the SiO$_2$/Si(111) substrate directly via molybdenum atoms, which were exposed outside after partial de-
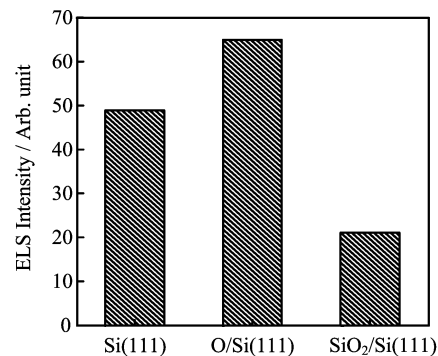
FIG. 3 The vibrational intensity of the C−O stretching mode of 5 L $Mo(CO)_6$ on clean Si(111), oxygen-precovered Si(111) and SiO$_2$/Si(111) at 100 K.

carbonylation of $Mo(CO)_6$. This adsorptive configuration of molybdenum subcarbonyls was also proposed for partially-decarbonylated $Mo(CO)_6$ on Rh(100) [46].

The HREELS intensity is correlated with not only the coverage of adsorbates, but also the adsorptive configuration of the surface adsorbed species. Due to the same adsorbates on these model surfaces, it is assumed that almost the same adsorptive configurations occur for molybdenum carbonyls. Therefore, the HREELS intensity can reflect the adsorbate coverage on the substrates. Figure 3 displays the vibrational intensity of the C−O stretching mode of 5 L $Mo(CO)_6$ on clean Si(111), O/Si(111) and SiO$_2$/Si(111) at 100 K. The vibrational intensity of the C−O stretching mode on O/Si(111) is much larger than that on clean Si(111). Owing to molecular adsorption of $Mo(CO)_6$ on both O/Si(111) and clean Si(111), the different vibrational intensities indicate that there are more adsorbates on the former than that on the latter. Oxygen adsorption maybe has a little modification effect on Si(111), consequently increasing the sticking coefficient of $Mo(CO)_6$ on O/Si(111). The vibrational intensity of the C−O stretching mode on SiO$_2$/Si(111) after 5 L exposure of $Mo(CO)_6$ at 100 K is smaller than half of that on clean Si(111). It is probably attributed to the partial decarbonylation of $Mo(CO)_6$ when exposed on SiO$_2$/Si(111) at 100 K, as discussed above. There are fewer carbonyl groups in molybdenum subcarbonyls than that in molybdenum hexacarbonyl, consequently less responsibility for HREELS measurements. Therefore, the vibrational intensity of the C−O stretching mode on SiO$_2$/Si(111) is remarkably smaller than that on clean Si(111), despite a stronger interaction of molybdenum carbonyls on the former than on the latter. Another reason might be the lower surface coverage of $Mo(CO)_6$ on SiO$_2$/Si(111) than on Si(111), which needs further investigation.

Our results clearly demonstrate different interactions of $Mo(CO)_6$ on clean and oxidized Si(111): a weak interaction occurs between adsorbed $Mo(CO)_6$ and clean Si(111), and $Mo(CO)_6$ molecularly adsorbs on clean
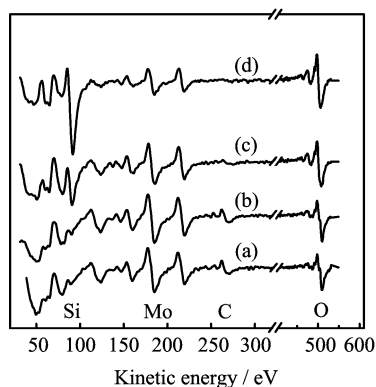
FIG. 4 Auger electron spectra of the SiO_2/Si(111) surface annealed at (a) 700 K, (b) 800 K, (c) 900 K, (d) 950 K, after exposure of 50 μPa $Mo(CO)_6$ for 30 min at substrate temperature of 700 K.

Si(111) at 100 K; precovered oxygen on Si(111) does not obviously affect the adsorptive property of $Mo(CO)_6$ on Si(111); however, a strong interaction occurs between adsorbed $Mo(CO)_6$ and SiO_2/Si(111), as a result, probably leading to the partial decarbonylation of $Mo(CO)_6$. Due to oxygen termination on the surface of SiO_2/Si(111), the CO, released from partial decarbonylation of $Mo(CO)_6$, has already desorbed from the substrates in our case at 100 K. It is also reported that no obvious CO desorption feature appears over the temperature range from 150 K to 700 K on SiO_2/Mo(112) model surface upon CO exposure of 4 L [47]. Molybdenum subcarbonyls were reported to undergo both desorption and further decarbonylation upon annealing at elevated temperatures [26, 48]. Therefore, it is likely to fabricate the Mo/SiO_2/Si(111) model catalyst by dosing $Mo(CO)_6$ at 100 K followed by annealing at higher temperatures, but the efficiency would be very low due to the competition between desorption and decomposition reactions. The efficient molybdenum deposition on the SiO_2/Si(111) surface is achieved by thermal decomposition of $Mo(CO)_6$ at a substrate temperature of 700 K under a $Mo(CO)_6$ pressure of 50 μPa for 30 min.

Figure 4 displays a series of Auger electron spectra taken from the sample annealed at elevated temperatures after molybdenum deposition at 700 K. The Mo Auger feature, corresponding to the MNN transitions, appears on the sample after $Mo(CO)_6$ exposure at 700 K. We also exposed the Si(111) substrate to $Mo(CO)_6$ of 50 μPa for 30 min at temperatures of 600−1000 K, but no signal for Mo was detected on the surface by means of AES. It is reasonable because $Mo(CO)_6$ could only molecularly adsorb on the clean Si(111) surface. Our HREELS results of $Mo(CO)_6$ adsorption on clean Si(111) upon annealing at elevated temperatures (not shown) clearly illustrate that the adsorbed $Mo(CO)_6$ does not undergo gradual decarbonylation, and directly desorbs molecularly from the Si(111) surface upon heating. Our observations are in

consistence with Bartosch et al.'s results [32] observing the desorption feature of $Mo(CO)_6$ at 205 K from the clean Si(111) surface. From the Auger feature of silicon, the substrate at 700 K is still the SiO_2/Si(111) surface. Additionally, some carbon is residual on the surface. These carbon contaminants on the deposited layers are the results of the dissociation of CO, catalyzed by Mo present on the surface [13]. With increasing substrate temperature, the Auger feature for the oxidized silicon reduces its intensity, while that for the zero-valent silicon increases. It is also noteworthy that the Auger signal for the residual carbon reduces its intensity as a function of sample temperature, and finally disappears upon annealing at 950 K. Simultaneously, the oxygen Auger signal decreases in intensity. It is caused by recombinative desorption of CO from the residual carbon and the surface oxygen. At the same time, it is very likely for the deposited molybdenum to capture the oxygen from the oxidized substrate upon high-temperature annealing. The Mo Auger feature gradually reduces its intensity with further increasing sample temperature, indicating desorption of the molybdenum component probably in the form of volatile MoO_3. Kummer also found that the MoO_3 could be volatilized merely above 973 K [49]. The desorption of the MoO_3 was observed on the ultrathin silicon dioxide films deposited onto the Mo(100) [50] and Mo(110) [51] substrates, where silicon dioxide was reduced by the molybdenum substrate to form volatile SiO and MoO_3. However, the desorption temperature of MoO_3 in the above SiO_2/Mo systems is 1400−1700 K, much higher than that in our case. In the SiO_2/Mo systems, the bulk molybdenum substrate is underlying the ultrathin silicon dioxide films, and stays in a compact stacking state; whereas in our case, the molybdenum nanoparticles are deposited on the oxidized substrate. The difference between these two cases causes the desorption temperature of MoO_3 to decrease to a large extent.

IV. CONCLUSION

Different interactions occur when $Mo(CO)_6$ was exposed on the clean Si(111) and SiO_2/Si(111) surfaces at 100 K, as detected by HREELS. At cryogenic temperature, a weak interaction occurs between adsorbed $Mo(CO)_6$ and clean Si(111), and $Mo(CO)_6$ adsorbs molecularly on the clean Si(111) surface; precovered oxygen on Si(111) does not affect the surface chemistry of $Mo(CO)_6$ on Si(111); however, a strong interaction occurs between adsorbed $Mo(CO)_6$ and SiO_2/Si(111), consequently probably lead to the partial decarbonylation of $Mo(CO)_6$. Therefore, employing $Mo(CO)_6$ as the precursor, metallic molybdenum could be successfully deposited on the SiO_2/Si(111) surface but not on the clean Si(111) surface. A portion of the metallic molybdenum is transformed into the MoO_3 on the SiO_2/Si(111) surface upon heating, and the evolved

MoO$_3$ finally desorbs from the substrate upon annealing at elevated temperatures. It is intrinsically instructional to prepare supported molybdenum-based catalysts efficiently and easily, without the surface carbon contaminant.

V. ACKNOWLEDGMENTS

[1] R. Psaro and S. Recchia, Catal. Today **41**, 139 (1998).
[2] C. Brémard, Coord. Chem. Rev. **178-180**, 1647 (1998).
[3] F. Zaera, J. Phys. Chem. **96**, 4609 (1992).
[4] M. D. Xu and F. Zaera, J. Vac. Sci. Technol. A **14**, 415 (1996).
[5] F. Zaera, Langmuir **7**, 1188 (1991).
[6] F. Zaera, Surf. Sci. **255**, 280 (1991).
[7] M. D. Xu and F. Zaera, Surf. Sci. **315**, 40 (1994).
[8] F. Zaera, J. Vac. Sci. Technol. A **7**, 640 (1989).
[9] F. Blanc, J. Thivolle-Cazat, J. M. Basset, C. Copéret, A. S. Hock, Z. J. Tonzetich, and R. R. Schrock, J. Am. Chem. Soc. **129**, 1044 (2007).
[10] F. Blanc, R. Berthoud, A. Salameh, J. M. Basset, C. Copéret, R. Singh, and R. R. Schrock, J. Am. Chem. Soc. **129**, 8434 (2007).
[11] M. B. Logan, R. F. Howe, and R. P. Cooney, J. Mol. Catal. **74**, 285 (1992).
[12] S. D. Djajanti and R. F. Howe, Stud. Surf. Sci. Catal. **97**, 197 (1995).
[13] Z. Q. Jiang, W. X. Huang, J. Jiao, H. Zhao, D. L. Tan, R. S. Zhai, and X. H. Bao, Appl. Surf. Sci. **229**, 43 (2004).
[14] Z. Q. Jiang, W. X. Huang, H. Zhao, Z. Zhang, D. L. Tan, and X. H. Bao, J. Mol. Catal. A **268**, 213 (2007).
[15] R. I. Nakamura, R. G. Bowman, and R. L. Burwell, J. Am. Chem. Soc. **103**, 673 (1981).
[16] R. I. Nakamura, D. Pioch, R. G. Bowman, and R. L. Burwell, J. Catal. **93**, 388 (1985).
[17] Z. Q. Jiang, W. X. Huang, Z. Zhang, H. Zhao, D. L. Tan, and X. H. Bao, Surf. Sci. **601**, 844 (2007).
[18] M. Kaltchev and W. T. Tysoe, J. Catal. **193**, 29 (2000).
[19] M. Kaltchev and W. T. Tysoe, J. Catal. **196**, 40 (2000).
[20] M. Kaltchev and W. T. Tysoe, Top. Catal. **13**, 121 (2000).
[21] Y. Wang, F. Gao, M. Kaltchev, D. Stacchiola, and W. T. Tysoe, Catal. Lett. **91**, 83 (2003).
[22] Y. Wang, F. Gao, M. Kaltchev, and W. T. Tysoe, J. Mol. Catal. A **209**, 135 (2004).
[23] Y. Wang, F. Gao, and W. T. Tysoe, J. Mol. Catal. A **235**, 173 (2005).
[24] Y. Wang, F. Gao, and W. T. Tysoe, J. Mol. Catal. A **248**, 32 (2006).
[25] M. Kurhinen, T. Venäläinen, and T. A. Pakkanen, J. Phys. Chem. **98**, 10237 (1994).
[26] C. C. Williams and J. G. Ekerdt, J. Phys. Chem. **97**, 6843 (1993).
[27] D. V. Chakarov, Z. C. Ying, and W. Ho, Surf. Sci. **255**, L550 (1991).
[28] L. J. Richter, S. A. Buntin, P. M. Chu, and R. R. Cavanagh, J. Chem. Phys. **100**, 3187 (1994).
[29] N. S. Gluck, Z. Ying, C. E. Bartosch, and W. Ho, J. Chem. Phys. **86**, 4957 (1987).
[30] Z. C. Ying and W. Ho, J. Chem. Phys. **94**, 5701 (1991).
[31] U. R. Schöffel, H. Rauscher, and R. J. Behm, J. Appl. Phys. **91**, 2853 (2002).
[32] C. E. Bartosch, N. S. Gluck, W. Ho, and Z. Ying, Phys. Rev. Lett. **57**, 1425 (1986).
[33] G. Hollinger and F. J. Himpsel, Phys. Rev. B **28**, 3651 (1983).
[34] J. Derrien and M. Commandré, Surf. Sci. **118**, 32 (1982).
[35] H. Ibach, H. D. Bruchmann, and H. Wagner, Appl. Phys. A **29**, 113 (1982).
[36] H. Ibach and J. E. Rowe, Phys. Rev. B **10**, 710 (1974).
[37] S. H. Lee and M. H. Kang, Phys. Rev. Lett. **82**, 968 (1999).
[38] S. H. Lee and M. H. Kang, Phys. Rev. B **61**, 8250 (2000).
[39] L. H. Jones, Spectrochim. Acta **19**, 329 (1963).
[40] L. H. Jones, J. Chem. Phys. **36**, 2375 (1962).
[41] L. H. Jones, R. S. McDowell, and M. Goldblatt, Inorg. Chem. **8**, 2349 (1969).
[42] C. Noguera, J. Phys.: Condens. Matter. **12**, R367 (2000).
[43] J. Goniakowski, F. Finocchi, and C. Noguera, Rep. Prog. Phys. **71**, 016501 (2008).
[44] Z. C. Ying and W. Ho, J. Chem. Phys. **93**, 9077 (1990).
[45] S. K. So and W. Ho, J. Chem. Phys. **95**, 656 (1991).
[46] T. A. Germer and W. Ho, J. Vac. Sci. Technol. A **7**, 1878 (1989).
[47] S. M. McClure, M. Lundwall, F. Yang, Z. Zhou, and D. W. Goodman, J. Phys. Chem. C **113**, 9688 (2009).
[48] K. P. Reddy and T. L. Brown, J. Am. Chem. Soc. **117**, 2845 (1995).
[49] J. T. Kummer, J. Phys. Chem. **90**, 4747 (1986).
[50] J. W. He, X. Xu, J. S. Corneille, and D. W. Goodman, Surf. Sci. **279**, 119 (1992).
[51] X. Xu and D. W. Goodman, Surf. Sci. **282**, 323 (1993).